Received: 4 July 2022 | Revised: 4 September 2022 | Accepted: 30 September 2022

DOI: 10.1002/jsp2.1228

RESEARCH ARTICLE

JOR Spine OPEN ACCESS

Homing of vertebral-delivered mesenchymal stromal cells for degenerative intervertebral discs repair – an in vivo proof-of-concept study

Jordy Schol[1,2] | Daisuke Sakai[1] | Takayuki Warita[2,3] | Tadashi Nukaga[1] | Kosuke Sako[1] | Sebastian Wangler[4,5] | Shota Tamagawa[1,6] | Stephan Zeiter[4] | Mauro Alini[4] | Sibylle Grad[4,7]

[1]Department of Orthopaedic Surgery, Tokai University School of Medicine, Isehara, Japan

[2]Research Center for Regenerative Medicine, Tokai University School of Medicine, Isehara, Japan

[3]TUNZ Pharma Co. Ltd., Osaka, Japan

[4]AO Research Institute Davos, Davos, Switzerland

[5]Department of Orthopaedic Surgery and Traumatology, Inselspital, Bern University Hospital, University of Bern, Bern, Switzerland

[6]Department of Medicine for Orthopaedics and Motor Organ, Juntendo University Graduate School of Medicine, Tokyo, Japan

[7]ETH Zürich, Institute for Biomechanics, Zürich, Switzerland

Correspondence
Daisuke Sakai, Department of Orthopaedic Surgery, Tokai University School of Medicine, 143 Shimokasuya, Isehara, Kanagawa 259-1193, Japan.
Email: daisakai@is.icc.u-tokai.ac.jp

Sibylle Grad, AO Research Institute Davos, Davos, Switzerland, Clavadelerstrasse 8, 7270 Davos, Switzerland.
Email: sibylle.grad@aofoundation.org

Funding information
AO Foundation; AOSpine; Bridging Grant from the Swiss State Secretariat for Education, Research, and Innovation, Grant/Award Number: BG03-092019

Abstract

Introduction: Cell transplantation shows promising results for intervertebral disc (IVD) repair, however, contemporary strategies present concerns regarding needle puncture damage, cell retention, and straining the limited nutrient availability. Mesenchymal stromal cell (MSC) homing is a natural mechanism of long-distance cellular migration to sites of damage and regeneration. Previous ex vivo studies have confirmed the potential of MSC to migrate over the endplate and enhance IVD-matrix production. In this study, we aimed to exploit this mechanism to engender IVD repair in a rat disc degeneration model.

Methods: Female Sprague Dawley rats were subjected to coccygeal disc degeneration through nucleus pulposus (NP) aspiration. In part 1; MSC or saline was transplanted into the vertebrae neighboring healthy or degenerative IVD subjected to irradiation or left untouched, and the ability to maintain the IVD integrity for 2 and 4 weeks was assessed by disc height index (DHI) and histology. For part 2, ubiquitously GFP expressing MSC were transplanted either intradiscally or vertebrally, and regenerative outcomes were compared at days 1, 5, and 14 post-transplantation. Moreover, the homing potential from vertebrae to IVD of the GFP^{+} MSC was assessed through cryosection mediated immunohistochemistry.

Results: Part 1 of the study revealed significantly improved maintenance of DHI for IVD vertebrally receiving MSC. Moreover, histological observations revealed a trend of IVD integrity maintenance. Part 2 of the study highlighted the enhanced DHI and matrix integrity for discs receiving MSC vertebrally compared with intradiscal injection. Moreover, GFP rates highlighted MSC migration and integration in the IVD at similar rates as the intradiscally treated cohort.

Conclusion: Vertebrally transplanted MSC had a beneficial effect on the degenerative cascade in their neighboring IVD, and thus potentially present an alternative administration strategy. Further investigation will be needed to determine the long-term

effects, elucidate the role of cellular homing versus paracrine signaling, and validate our observations on a large animal model.

KEYWORDS
cell therapy, degeneration, homing, intervertebral disc, mesenchymal stromal cells, rat model

1 | INTRODUCTION

Low back pain (LBP) stands as the primary cause of disability,[1] and contemporary treatment procedures remain inadequate for a large portion of LBP patients.[2] Upcoming regenerative therapeutic strategies, for example, gene therapy,[3,4] tissue engineering,[5–7] biomaterials,[8] and growth factor treatments,[9] are highly anticipated as methods to alleviate pain associated with intervertebral disc (IVD) degeneration.[10] Particularly, cell therapy has been proposed as a promising technique towards supporting IVD repair[11] and has shown rapid developmental progression[12–14] with multiple clinical trials highlighting the potential of cell injection to augment IVD imaging modalities.[15] The regenerative effects of the de novo cells are expected to be derived from either direct incorporation into the IVD and their local contribution to disc matrix reorganization.[15] Alternatively, the cells can stimulate or attract host cells to in turn support a more anabolic disc environment.[15] Despite promising preclinical and preliminary clinical results, concerns and questions remain regarding optimal cell products and transplantation strategies.[16–18] One critical controversy lies with the limited nutrient and oxygen availability in the largely avascular IVD,[19] which is further compromised as part of the degeneration cascade.[20] In silico models have highlighted the importance of cellular density and their constraints on disc nutrition.[21,22] Another concern is the method employed to introduce the therapeutic cells into the disc interior. Specifically, most reported clinical studies employ intradiscal injection of their cell products using a 21- or 22-gauge needle.[12] The needle puncture introduces additional impairment to the integrity of the IVD, presenting additional damage for the cells to surmount. A 10-year follow-up matched-cohort study, highlighted that disc needle puncture as part of discography procedure accelerates disc degeneration.[23] Moreover, disc puncture has been employed in multiple animal studies as a method to induce a degenerative IVD cascade.[24–27] Cumulatively, these facts highlight the potential detrimental effects of intradiscal needle puncture. Finally, successful implantation of the cell product is another challenging aspect, as integration of the cell product might be limited by the high intradiscal pressure and mechanical strains imposed on the fibrocartilage joint. This could cause the transplanted products to leak out either through fissures in the degenerating discs or through the newly created hole formed by the needle insert. The extruded cells could thereby compromise other tissues or form undesired tissue structures elsewhere, for example, osteophyte, as observed in the work of Vadalà et al.[28] Altogether, the intradiscal injection of large quantities of cells is linked with a variety of restrictions and concerns, thus justifying investigation into alternative transplantation strategies.[29]

Interestingly, a variety of studies have highlighted the potential of cells to migrate towards and into degenerating IVD over the disc endplates.[30] Particularly, mesenchymal stromal cells (MSC) show a strong homing affinity towards damaged or diseased tissues.[31] Moreover, MSC have been shown to alleviate discogenic pain and support improvement on MRI modalities in some reported clinical studies.[15] Whole IVD organ culture studies have shown the active migration of MSC seeded on top of their cartilaginous endplates, which was further enhanced in degenerating IVD.[32–34] Moreover, the newly integrated cells were shown to enhance production of growth factors known to stimulate extracellular matrix (ECM) synthesis, for example, fibroblastic growth factor (FGF)-6 and FGF-7, increase the expression of aggrecan and type II collagen in the nucleus pulposus (NP) of the IVD,[32] and enhance the $Tie2^{+}$ progenitor cell[35,36] population in the NP.[34] In vivo models have highlighted the potency of this homing mechanism, as green fluorescent protein (GFP) labeled MSC were shown capable of migrating into the IVD interior from bone marrow sources in a tail-loop degeneration mouse model.[37] These cellular features could potentially be exploited to engender a de novo and regenerative cell population into degenerating IVD or otherwise help support disc repair via paracrine signaling without the need for puncturing the disc. As such, the aim of this proof-of-concept study was to examine, in a coccygeal disc degeneration rat model, the administration of MSC at close proximity to the IVD as a potential strategy for limiting induced disc degeneration.

2 | METHODS AND MATERIALS

2.1 | Study design

Each experiment involving animal models was reviewed and approved by Institutional Review Board for Clinical Research at Tokai University for safe animal experimentation, under application number 214033. The study involved two separate animal studies (Figure 1B,C), examining the regenerative potential of vertebral MSC transplantation on degenerating IVDs in part 1, and the migration potential of the vertebral transplanted MSC in part 2. Moreover, in part 1, we examined the potential of tail irradiation to assess its potential for enhancing cell transplant efficacy. For both transplantation studies, female Sprague Dawley (SD) rats (MIZUSETSU, Japan) were employed and housed in pairs with ad libitum access to food and water and controlled day/night cycles. For both parts, the transplantation product was concealed to the performing surgeon, and conditions were randomly assigned to disc levels using the rand-function in Microsoft Excel (Microsoft corp., USA).

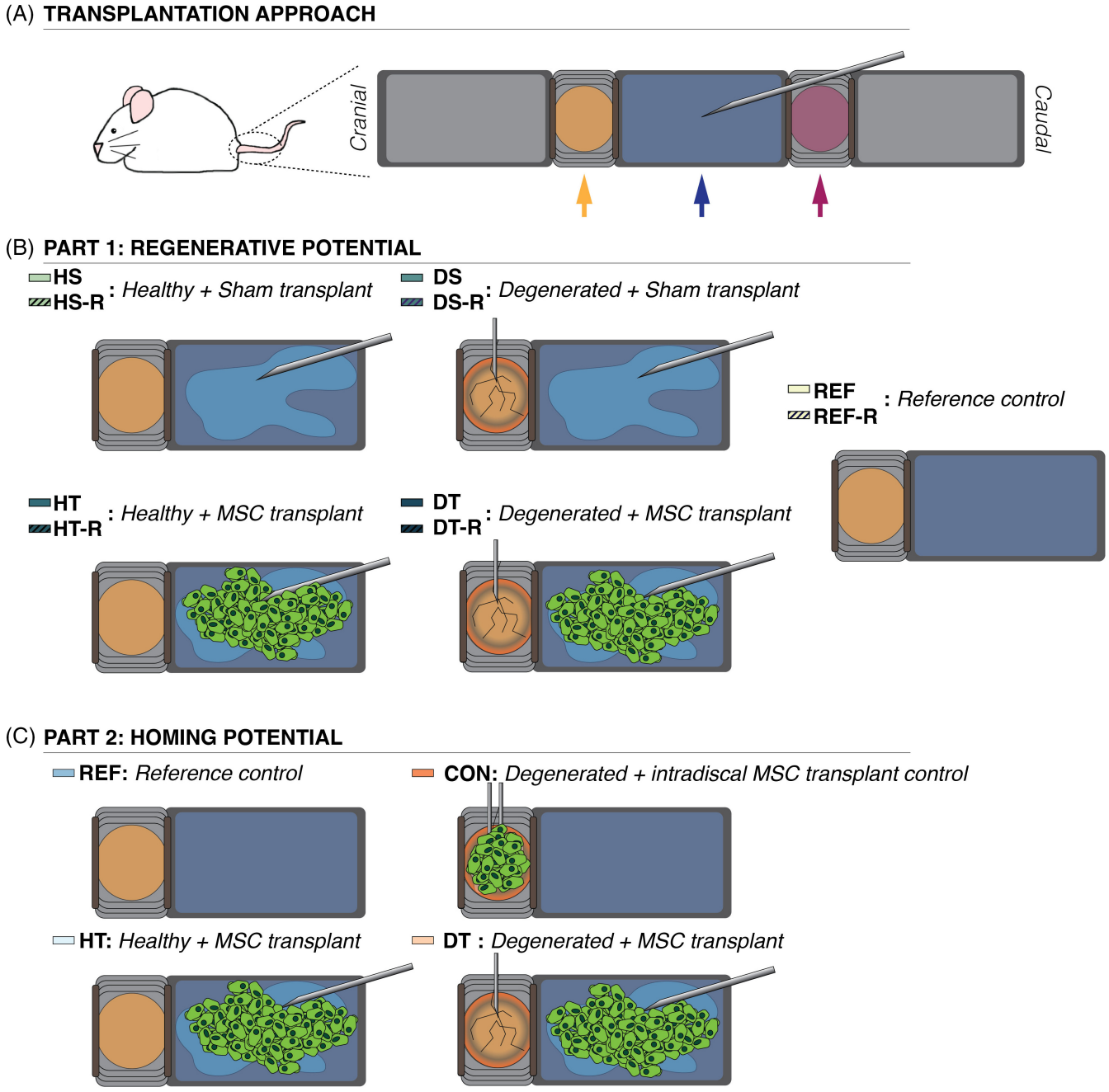

FIGURE 1 Study design overview. (A) Vertebral transplantation methods involving the introduction of transplant products into the interior of the vertebra (blue arrow) by sacrificing the caudal disc (maroon arrow) to assess the potential effect on the experimental disc (orange arrow) in a rat coccygeal disc degeneration model. (B–C) Overview of experimental conditions examined for part 1 (B) or part 2 (C) of the study, which involved a healthy disc or disc subjected to induced disc degeneration by nucleus pulposus tissue aspiration and transplantation of either PBS or MSC containing PBS into the vertebra or intervertebral disc. Indicated colors for each condition are applied throughout the article. Abbreviations: MSC, mesenchymal stromal cells; "-R", irradiated cohort; PBS, phosphate buffered saline.

2.2 | PART 1: Vertebral transplanted MSC induced IVD regeneration

2.2.1 | Cell Isolation and Expansion

For the first part of the study, two male SD rats (11-weeks-old) were sacrificed under 2.5% isoflurane (Pfizer, USA) inhalation and by injection of 150 mg/ml cardiac pentobarbital (Tokyo Chemical Industry, Japan). Both tibias and femurs were explanted and soft tissue was removed. Following the work of Zhang & Chan[38] both ends of the bone specimens were cut off and using a 23G needle, bone marrow content was extracted by flushing the interior with DMEM (Gibco, USA) containing 10% (v/v) FBS (SIGMA, Japan). Obtained cells, were expanded in "Mesenchymal stem cell medium

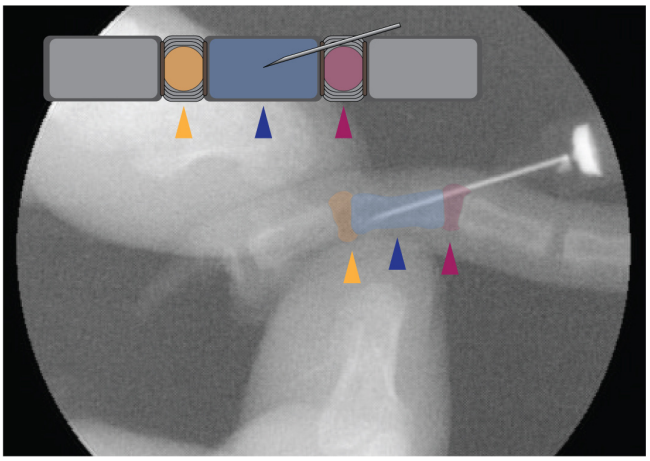

FIGURE 2 Surgical procedure. Radiographic representation of needle puncture and transplantation into the interior of the vertebra, via the caudal IVD, to transplant 10 µl of transplant product, for example, contrast agent. Images obtained from post-mortem rat tail waste material obtained from unrelated study. For full transplantation procedure see Figure S3. Orange: experimental disc, blue: vertebral transplantation site, and pink: sacrificial disc to enable needle insert into the vertebra.

2" (Promocell, Germany) under 21% O_2 up to two passages prior to transplantation.

2.2.2 | Surgical procedures

Starting 2 days prior to surgical intervention, a total of 24 female SD rats (17-weeks-old at 324 [±20] gram) were treated daily with 0.20 mg/kg tacrolimus hydrate (Astellas Pharma Inc., Japan) for a period of 12 days. Twelve of the 24 rats were assigned to an irradiated group (indicated with "-R") and these were subjected to 6 Gy of radiation at approximately 0.55 Gy/min, specifically focused on the tail, 1 day prior to the transplantation. This was employed with the hypothesis that irradiation could increase the likelihood of transplanted MSC engraftment by reducing competition with a variety of other endemic vertebral bone marrow cells. The rest of the body was protected from the radiation beams. Next, in all rats, under continuous 2.5% isoflurane (Pfizer, USA) inhalation, coccygeal discs 1/2, 3/4, 5/6, 7/8, and their caudal vertebrae 2, 4, 6, and 8 respectively, were randomly assigned one of four conditions. (Figure 1B) All coccygeal discs from Co1/2 to Co8/9 were surgically exposed. Under fluoroscopic guidance (Figure 2), two IVDs were subjected to induced disc degeneration, by aspiration of approximately 10 µl NP tissue through a 23G needle and 10 ml syringe. Transplantation of either 10 µl of PBS or 10 µl 2.5 × 10^5 MSC in PBS, was performed by creating a defect in the caudal vertebrae with a 18G needle. Specifically, the needle was inserted through the AF of the coccygeal IVD 2/3, 4/5, 6/7, and 8/9 in a cranial direction in order to enter the interior of coccygeal vertebrae 2, 4, 6, and 8 respectively. (Figures 1A and 2) The 18G needle was retracted and through the defect, via 27G needle, 10 µl of the transplant product was administered at close proximity to the endplate of the IVD of interest. Either 10 µl of PBS was injected next to a healthy IVD (HS condition) or disc induced to degenerate (DS condition). Alternatively, MSC were transplanted next to a healthy IVD (HT condition) or degenerating IVD (DT condition). Disc Co9/10 remained unmanipulated and functioned as a healthy reference control (REF condition). All conditions in the irradiated cohort followed an identical approach and are indicated by an "-R", that is, HS-R, DS-R, HT-R, DT-R, or REF-R respectively. Thereafter, incisions were sutured, 0.05 mg/kg Lepetan (buprenorphine HCL; Otsuka Pharmaceutical, Japan) was administered, and body weight was tracked daily throughout the study. Radiographic images were obtained from the coccygeal region of interest at the time of transplantation, as well as 2 weeks ($n = 24$), and 4 weeks ($n = 12$) post-surgery.

2.2.3 | Tissue explantation and processing

Two- or four-weeks post-transplantation the respective rats were sacrificed under 2.5% isoflurane (Pfizer, USA) inhalation and by injection of 150 mg/ml cardiac pentobarbital (Tokyo Chemical Industry, Japan). From each rat, all 5 IVDs of interest with their caudal vertebrae were collected as one sample and placed in 4% paraformaldehyde at 4°C. Subsequently, the specimens were subjected to 70, 80, 96, 80, 70% (V/V) ethanol, for 12 h each, followed by WAKO decalcification solution A (WAKO, Japan) for 18 h, and 5% sodium sulfate for 12 h. Finally, samples were dehydrated by 70, 80, 96, and 100% (V/V) ethanol and xylene. Samples were placed in paraffin blocks and 8 µm sections were obtained using a Yamato REM710 microtome (Yamato Kohki Industrial Co. LTD., Japan) for histological examination.

2.3 | PART 2: Optimized procedures for MSC tracing

2.3.1 | Cell Isolation and Expansion

For the second part, two transgenic male mice (1-year-old) that ubiquitously expressed GFP were kindly gifted by Professor Yutaka Inagaki (Dep. Innovative Medical Sciences, Tokai University School of Medicine, Japan). The mice were sacrificed through cervical dislocation and under sterile conditions both femurs and tibias were explanted. Following instruction from Zhu et al.[39] compact bone derived MSC were isolated, cultured using MesenCult™ (Mouse) (STEMCELL Technologies Inc., Canada) following the manufacturer's instructions, and expanded under 5% O_2 for up to two passages prior to usage in the transplantation procedures.

2.3.2 | Surgical procedures

For the second part, 2 days prior to surgical intervention, a total of 20 female SD rats (11-weeks-old at 231 [±12] gram) were similarly

treated with tacrolimus hydrate. Rats were randomly allocated to 0-days ($n = 2$), 1-day ($n = 5$), 5-days ($n = 5$), or 14-days ($n = 7$) cohort. Each rat tail was subjected to three experimental and one control condition (see Figure 1C). All coccygeal discs ranging from 2/3 to 7/8 were exposed. Coccygeal discs 2/3 or 5/6 were randomly allocated to the HT or DT condition, and 4/5 and 7/8 were randomly assigned REF or as an intradiscal transplantation control (CON). Specifically, discs assigned as DT and CON conditions were subjected to 10 µl NP tissue aspiration with a 23G needle. 10 µl PBS with 2.5 $\times$ 10^5 MSC were transplanted directly into the interior of the vertebrae coccygeal level 3 and 6 using a 27-gauge needle (see Figures S2 and S3). Alternatively, 10 µl of 1.0 $\times$ 10^5 MSC were transplanted into the IVD assigned as the CON. Thereafter, incisions were sutured, rats received 0.05 mg/kg Lepetan (buprenorphine HCL; Otsuka Pharmaceutical, Japan), and body weight was tracked daily throughout the study. Radiographic images were obtained from the coccygeal region at the time of transplantation and 5-, 10-, and 14-days post-surgery.

2.3.3 | Tissue explantation and processing

Following the assigned cohorts, rats were sacrificed under 2.5% isoflurane (Pfizer, USA) inhalation and by cardiac injection of 150 mg/ml pentobarbital (Tokyo Chemical Industry, Japan). For each time-cohort, the disc explants from three rats were processed for sagittal plane sections and two rats were processed for axial plane sections. (1:1 for the 0-day cohort) Note that, the explants from two rats in the 14-day cohort were used for experiments outside this report, and were not processed for histology or immunohistochemistry. Sagittal and axial plane samples were both fixed in 4% PFA for 4 days and processed through ethanol solutions as previously described. Sagittal samples were thereafter decalcified in the gentler WAKO decalcification solution B (WAKO) for 4 weeks, with a weekly refresh of the reagent. The samples were thereafter cut throughout the center of the disc in the sagittal plane. Axial processed samples, were not decalcified but instead directly cut through the center in the axial plane. Both sagittal and axial samples were incubated in 10 (W/V), 20 (W/V), and 30% (W/V) concentration of sucrose solution for 24 h each, and then snap frozen in Tissue-Tek® O.C.T. compound (Sakura Finetek Japan Co., Ltd., Japan). Cryosections were thereafter prepared at 8 µm using a Leica CM3050 S cryostat (Leica Biosystems, Germany) and applied for histological and immunohistochemistry staining.

2.3.4 | Radiographic assessment

For both the first and second part, radiographic images were obtained from the coccygeal region from a left-lateral approach using a fluoroscopic imaging intensifier DHF-105CX (Hitachi, Tokyo, Japan). In a blinded manner disc height index (DHI) was calculated as previously described[40] and normalized to the DHI pre-transplantation.

2.3.5 | Histology, immunohistochemistry, and histological scoring

Paraffin- and cryo-sections were stained by hematoxylin/eosin (HE) or 1 g/L Safranin-O (Merck, Kenilworth, New Jersey, USA) 800 mg/L Fast Green FCF staining (Merck) solution. Paraffin sections were thereafter captured by KEYENCE fluorescence microscope BZ-9000 (Keyence Ltd., Japan) and digitally merged via imaging stitching. Cryosections were captured through an Olympus IX70 microscope (Olympus, Tokyo, Japan). Subsequently, for part 1 all sections were independently and blindly scored by two researchers (J.S. & S.T.) according to the rat-specific classification set out in Lai et al.[25] For cryosections in part 2, scores were focused on NP-size, area, cell number, cell morphology, and NP-AF border categories.

2.3.6 | GFP tracing by immunohistochemistry staining

Immunohistochemical staining targeting GFP was employed to assess the ability of the GFP^+ MSC to migrate into the IVD at all time points. Cryosections were rehydrated in 0.01 M PBS for 10 min, followed by digestion with 50 mU Chondroitinase-ABC (Sigma-Aldrich, USA) for 30 min at 37°C. Samples were washed and blocked with 0.1% (v/v) Triton-X (Sigma-Aldrich), 3% BSA, PBS for 30 min at room temperature. Subsequently, sections were subjected to 1:500 polyclonal rabbit anti-GFP antibody (Ab290, Abcam) at 4°C overnight. The next day, samples were washed and stained through secondary goat anti-rabbit conjugated with Alexa633 (A21071, Abcam) for 1 h at room temperature. Finally, samples were washed and mounted with VECTASHIELD HardSet Mounting Medium with 40 6- diamidino-2-phenylindole (DAPI) (Vector Laboratories USA). Sections were directly assessed and photographed by LSM 510 META confocal microscope (ZEISS, Germany). Pictures were captured while being blind to the condition. Each section was photographed at 9 distinct regions of interest (ROI) depending on the cutting-plane (See Figure 5A,B). GFP was detected both at emission of 488 nm (natural GFP) and 633 nm (immunohistochemical label). The tally of cell was performed for each ROI using Image J 1.53 (National Institutes of Health, USA). Only cells presenting complete DAPI staining were included in the count. Cells were considered GFP^+ only if a $DAPI^+$ nucleus corresponded with fluorescent intensity at the 488 nm and 633 nm region, in order to prevent false positives. The total cells per ROI were determined by each DAPI spot and used to calculate the rate of GFP^+ cells. GFP^+ rates were determined for the entire IVD as well as for the inner-AF + NP (Sagittal ROI: c-h, Axial ROI: e-i) and outer-AF (Sagittal ROI: a,b,i, and g, Axial ROI: a-d; see Figure 5A,B).

2.3.7 | Statistics and visualization

Significance for non-temporal assessments were performed by one-way analysis of variance (ANOVA) followed by Tukey's multiple comparisons. Temporal assessments were determined by unpaired

ordinary two-way ANOVA and corrected by Tukey's multiple comparisons test. Normality was assessed through Shapiro–Wilk test. All graphical images and statistical analysis are obtained via Prism GraphPad v7.0c (GraphPad Software Inc., USA). All values are presented as mean values (±SD). Differences of $p < 0.05$ were considered statistically significant. Illustrations were designed using Adobe Illustrator version 26.0.3 (Adobe Inc., San Jose, California, USA).

3 | RESULTS

3.1 | PART 1: Vertebral transplanted MSC induced IVD regeneration

3.1.1 | General findings

No complications were observed as part of the study. The surgeries took on average 30.4 min (±8.4 min) per rat. Tracking of body weight revealed a sharp decline of 8.6% (±1.7) in relative bodyweight the day after transplantation to a maximum decline of 10.5% (±2.7%) at day 4 post-transplantation after which a trend of increased bodyweight was observed. (Figure S1) No differences could be observed in body weight changes when comparing the irradiated (-R) to non-radiated groups.

3.1.2 | Disc Height Index assessment

Two weeks after degeneration induction the DS and DS-R condition revealed a significant ($p < 0.001$) decrease in DHI compared to pre-operative DHI, suggesting successful degeneration induction. (Figure 3A) All healthy conditions (i.e., REF, REF-R, HS, HS-R, HT, and HT-R) showed maintenance of DHI compared to their pre-operative conditions, and were significantly higher compared to the DS or DS-R conditions at both time points. DT and DT-R resulted in a significant improvement in DHI compared to the DS ($p = 0.003$) and DS-R ($p = 0.001$) controls respectively at week 4. (Figure 3A).

3.1.3 | Histological and histological scoring

General histological observation highlighted the maintenance of IVD not induced to degenerate, while overall DS and DS-R showed clear disorganization in AF and NP matrix structures. DT and DT-R conditions showed more mixed results, but were generally able to retain parts of the IVD organization. (Figure 3B) Specifically, histological outcomes scored via the ORS Spine classification system[25] confirmed the successful induction of disc degeneration, as all healthy conditions maintained healthy IVD features, while the DS and DS-R presented significant

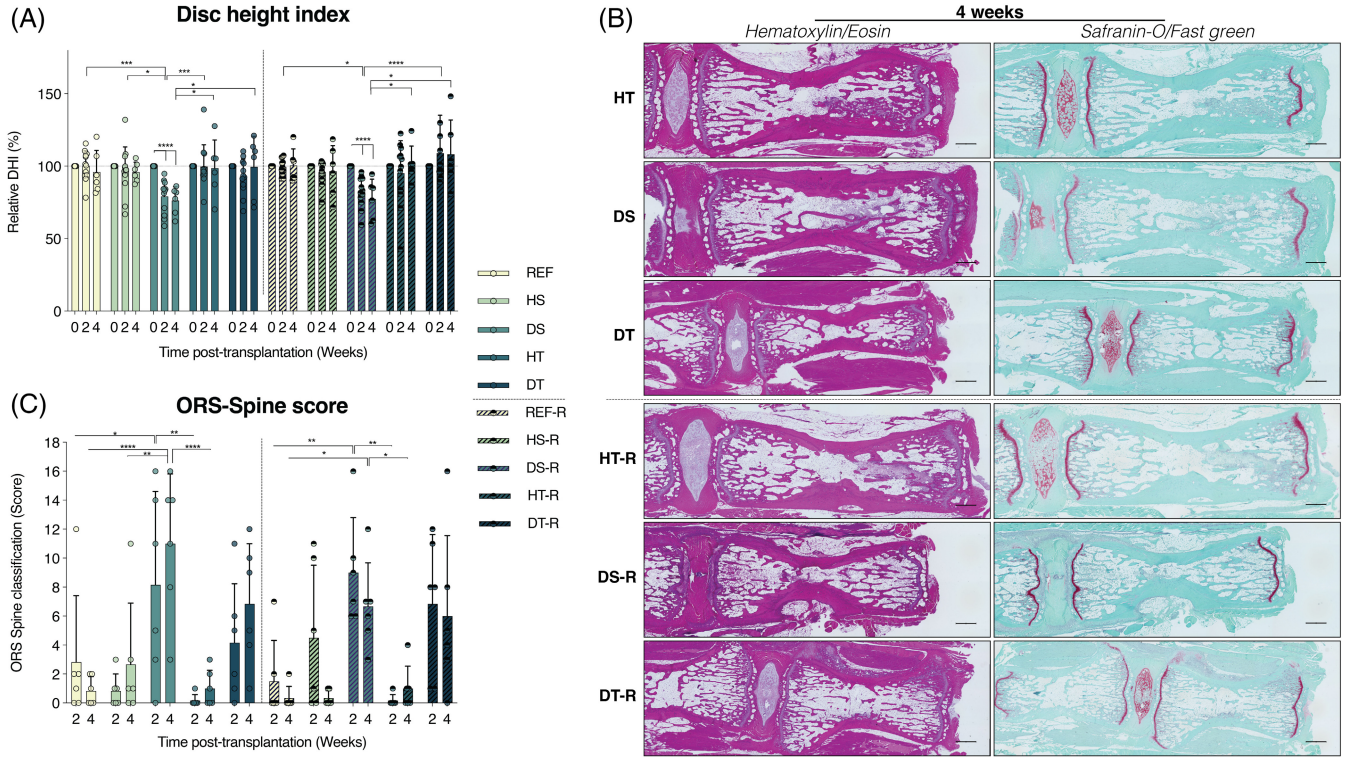

FIGURE 3 Overview of primary outcomes part 1; Regenerative assessment. (A) Relative disc height index (DHI) evaluations of all conditions determined at 2-weeks ($n = 12$) and 4-weeks ($n = 6$) post-transplantation as a percentage of pre-transplantation DHI. (B) Examples of histological specimen of IVD and vertebra explants from week 4 cohort stained through hematoxylin/eosin or safranin-O/fast-green. Scale bars represent 1000 μm (C) Histological scoring of explants ($n = 6$) using the full ORS Spine rat histopathology classifications scheme. Maximum score of 16 indicates severe degeneration and a minimum score 0 indicates a non-degenerative disc. For group classification please see Figure 1. Bars represent averages, error bars represent standard deviations, and circles indicate average individual measurements/scores. *$p \leq 0.05$, **$p \leq 0.01$, ***$p \leq 0.005$, and ****$p \leq 0.001$. "-R" indicates irradiated groups.

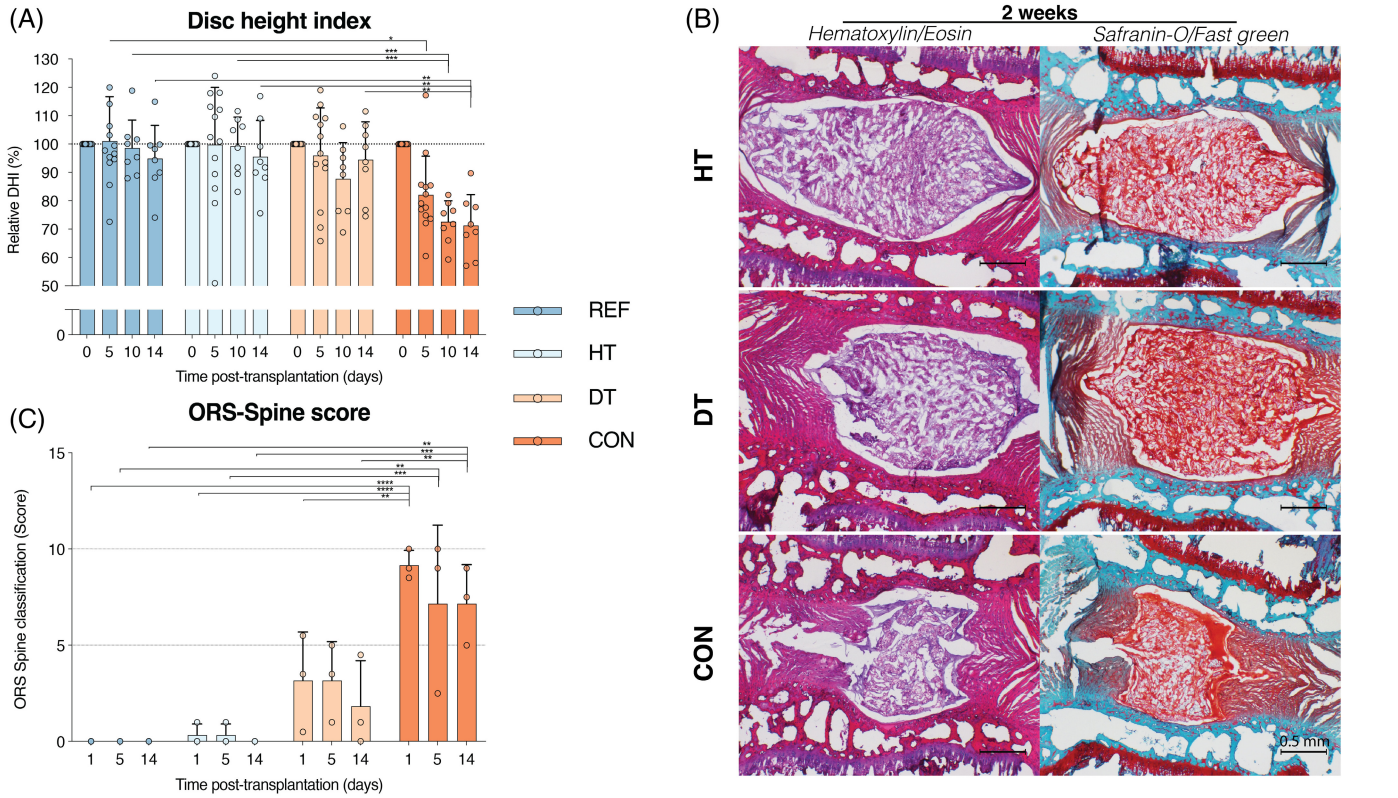

FIGURE 4 Overview of outcomes part 2; Homing potential. (A) Relative disc height index (DHI) evaluations of all conditions determined at each time-point of the 2-week observation period, presented as a percentage of pre-transplantation DHI. (Day 5: $n = 13$, day 10 and 14: $n = 8$). (B) Representation of histological observations from the 2 weeks observation period. Scale bars represent 500 µm. (C) Histological ORS-Spine classification outcomes for the nucleus pulposus categories. ($n = 3$) Bars represent averages, error bars represent standard deviations, and circles indicate average individual measurements/scores. $^{*}p \leq 0.05$, $^{**}p \leq 0.01$, $^{***}p \leq 0.005$, and $^{****}p \leq 0.001$.

worsening in histological features. The DT condition showed an increasing trend in histological scoring; nonetheless, the scores were neither significantly worse than the REF, HS, or HT conditions, nor showed significant improvement compared to the DS condition, overall suggesting at most a trend of limiting the induced degeneration compared to DS. Similarly, the DT-R condition showed neither significant worsening compared to REF-R, HS-R, or HT-R nor a significant improvement compared to DS-R. The beneficial trend was less evident for the DT-R condition. A breakdown of the scoring categories (Figure S4) revealed differences were mainly resulting from changes in NP and AF-lamellar organization.

3.2 | PART 2: Optimized procedures for MSC tracing

3.2.1 | General observations

Isolated and expanded murine MSC were confirmed to express GFP. (Figure S1) Transplant volume retention was confirmed effective on post-mortem rat tail tissue obtained from an unrelated study; 10 µl contrast agent could successfully be implanted into the vertebra interior without evidence of leakage. (Figures S2 and S3) Body weight measurements revealed a slight decrease following the transplantation procedure, but quickly recovered and kept increasing onwards. (Figure S1) No significant adverse events were recorded. Average surgery time was recorded at 10.8 ± 5.2 min.

3.2.2 | Disc height index measurements

DHI evaluations revealed maintenance of disc height for the healthy conditions (REF, HT) overtime. (Figure 4A) Interestingly the intradiscal injection of MSC showed a continuous decline in DHI resulting in significant DHI loss compared to the REF and HT conditions at day 10 and 14, with a loss of approximately 27.5%. Again, DT conditions were able, in part, to limit the decline in DHI, presenting a relative DHI at day 14 of 95.5%, significantly higher than the CON condition. ($p = 0.0097$).

3.2.3 | Histological observations and scoring

Histological scoring of NP features through the ORS Spine classification[25] showed maintenance of the healthy REF and HT conditions. (Figure 4B,C) The CON showed incapable of preventing disc degeneration, as highlighted by a significantly higher score compared to the REF and HT conditions from day 1, which further deteriorated at each

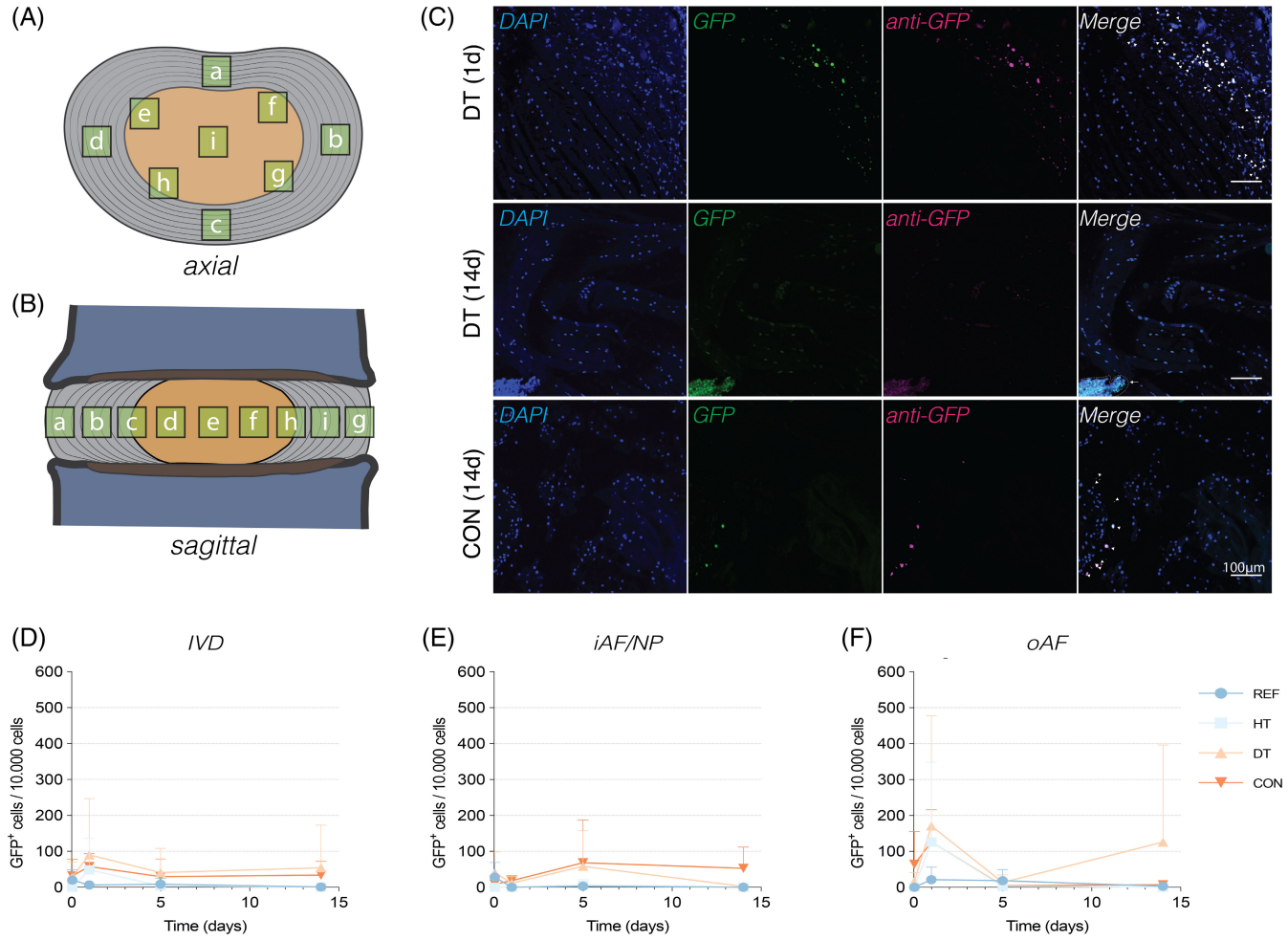

FIGURE 5 Overview of MSC tracing assessment. (A) Overview of region of interest (ROI) captured in axial-plane sections and (B) sagittal plane sections. (C) Examples of detected GFP^+ cells. Arrowheads indicate GFP^+ cells, arrow indicates a cluster of GFP^+ cells, scale bar represents 100 µm. (D) Rate of detected GFP^+ cells per disc indicated as positive cells per 10.000 cells. (E-G) Average rate of GFP^+ cells/ 10.000 cells detected in each disc indicated for (E) the complete IVD, (F) inner annulus fibrosus with nucleus pulposus (iAF/NP), or (G) outer annulus fibrosus (oAF). ($n = 5$, day 0: $n = 2$).

time point. The DT condition showed overall lower scores than the CON conditions, and was not significantly higher than the REF or HT conditions. Crucially, the DT condition had a significantly better score compared to the CON condition at day 1 ($p = 0.004$) and day 14 ($p = 0.009$), resulting in an average of five-point improvement at day 14. For deconstruction of the histological scores see Figure S5.

3.2.4 | GFP tracing and counting

GFP-expressing and GFP-immunostained cells could be detected in a small set of samples (Figure 5C), although overall detection rates were low. No significant differences were found between the different conditions, although DT and CON cohorts presented a trend of higher GFP^+ rates compared to REF and HT. (Figure 5D) Cumulatively, more GFP^+ cells were observed in DT and CON cohorts, than REF and HT conditions, although these findings were not exclusive to DT and CON conditions. (Figure 5D–F) For example, GFP+ cells were detected in HT conditions as well as REF samples; suggesting the ability of MSC placed in the highly vascularized vertebrae to migrate beyond the scope of their neighboring IVDs. Moreover, GFP^+ cells were detected at higher rates in the outer AF compared to the inner-AF and NP regions, although this might in part be due to the overall lower cell count in the outer AF. (Figure 5D–F) Reported numbers were consistent for all time points.

4 | DISCUSSION

Cell therapy is a rapidly progressing technology, that has been demonstrated strikingly effective in an array of disc degeneration animal models[41] and is showing its first potential effects on alleviating pain and improving disc MRI features in clinic trials.[15] Our study explored an alternative strategy to implant therapeutic cells to engender a regenerative effect on induced disc degeneration. Here our results indicate that the introduction of MSC in the vertebra, in close

proximity to a degenerating IVD, can prevent or delay some aspect of the degenerative cascade. Specifically, DHI was retained in observation period of at least 1 month, and quality of IVD tissue also presented a trend of improvement. Most striking was the significant improvement in DHI retention for discs neighboring vertebrally transplanted MSC, compared to IVD treated by intradiscal injection as done clinically. It should however be noted, that the CON condition was subjected to disc puncture twice; one 23G needle puncture for NP aspiration as part of degeneration induction and one 27G needle puncture for the MSC transplantation. Issy et al.[42] emphasized that even a 30G needle can promote a significant degenerative cascade in rat IVD. As such, interpretation of our findings requires caution. Regardless, our data do raise some questions with regard to the efficacy of intradiscal MSC injection. Additionally, for part 1 of the study, tail-specific irradiation was employed with the rationale to reduce the number of active cells in the vertebrae thereby enhancing the likelihood of transplanted MSC to integrate. Nevertheless, this speculated optimization did not proof beneficial, as DHI and histological changes remained similar between irradiated and non-irradiated cohorts. Interestingly, however, the cell number and cell morphology scores (Figure S4) generally showed lower scores for the irradiated discs than the non-radiated samples. Additionally, our study employed tacrolimus hydrate as an immunosuppressive drug for the allogenic- and xenogeneic MSC transplantation. This drug functions primarily through inhibiting calcineurin phosphatase thereby dysregulating interleukin 2 expression, restricting T-cell activation and migration.[43] Nevertheless, tacrolimus has also been shown to effectuate other cellular processes, for example, interfering in fibrosis[44,45] and promotion of osteogenesis.[46] As such, how this drug might have impacted the migratory and regenerative potential of the vertebrally transplanted MSC remains to be determined.

Our results confirmed our previous findings in multiple ex vivo organ-culture studies, that MSC have the intrinsic capacity to migrate over the endplate and into the IVD.[32–34,47] Moreover, our study similarly suggest an initial trend of enhanced affinity of MSC towards degenerating discs contrary to healthy discs, as highlighted by the higher number of GFP^+ cells detected in the DT cohort compared to HT. Again, this suggests that chemotactic factors secreted by NP and/or AF cells in part are able to promote the migration of MSC into the IVD. Previous reports have highlighted the predominant role of Stromal Cell-Derived Factor 1α (SDF1α),[48] C-C Motif Chemokine Ligand 5 (CCL5),[49] and C-X-C chemokine 6 (CXC6)[49] as chemokine factors secreted from degenerating IVD tissues and capable of enhancing cell migration. Complementary, expression of the C-X-C chemokine receptor 4 (CXCR4) has shown to be essential for MSC homing.[50] With respect to the IVD, work by Wangler et al. highlighted that MSC attracted by CCL5 expressed high levels of the surface marker CD146.[47] Moreover, the $CD146^+$ MSC subpopulation, presented higher glycosaminoglycan production rates than $CD146^-$ populations. Overall, these studies highlight, that specific MSC subpopulations are 1. more inclined to migrate towards degenerating IVD and 2. present higher regenerative potential for IVD-ECM production. In our study, no optimization of the MSC transplantation product was employed. As such, future experiments could focus on optimizing the cell product, by selecting an optimal combination of migratory and regenerative cells through cell sorting[36,47] or employing cell priming techniques.[31,51,52]

Although our study showed a trend of enhanced MSC migration into degenerating IVD, the overall rate of GFP^+ cells detected was generally low. The study was specifically designed to optimize detection rates of GFP^+ cells, through employing gentle decalcification (via EDTA) and frozen sections, to limit GFP protein denaturation and background staining from paraffin. Combined with our double positivity approach (natural GFP detection and through immunofluorescence staining) tracing could be reliably performed and limited the risk of false positive observations. Nonetheless, the counted numbers remained small, with many of the discs showing no GFP^+ cells within the IVD environment, suggesting only a fraction of the transplanted MSC migrated into the IVD. Moreover, detection rates were also low for the CON conditions. These observations support previous suggestions that intradiscally transplanted cells show an overall low rate of retention and survival.[13] Notably, however, we did not encapsulate the cells in any adherent carrier, which could have increased the retention and prevent potential cell leakage. Also, for the vertebral cell transplantation, the caudal IVD was sacrificed to enable the needle to enter the vertebral interior. As such, it is very likely that this defect also had an attractive potency to the transplanted MSC, and might have reduced the rate of MSC migration observed in our study. Finally, the xenogeneic nature (murine to rat; part 2), male to female (part 1 & 2), and general allogenic transplantation mode (part 1) could have limited the overall survival and integration of the transplanted cells, despite immunosuppression through tacrolimus hydrate administration.[43] Notwithstanding the limited migration rates, regenerative effects were still observed. Whether the outcomes are resulting from a small number of migratory cells or are the result of paracrine signaling, remains to be determined. (Figure 6) MSC and NP cell co-culture set-ups have highlighted the regenerative potential of MSC derived paracrine factors and exosomes on promoting NP cell anabolism.[53–56]

For our study, we employed a needle insert via a sacrificial IVD into the vertebra. This approach was considered optimal for this small animal model. For larger vertebral bodies in human or large animal models, alternative vertebral transplantation strategies can be considered. For example, the creation of a drill hole from a lateral approach could enable the transplantation of MSC into the vertebra. Initial testing on post-mortem rat tail (see Figure S2) confirmed the validity of the approach, although the defect was considered too large for the small rat model. However, this approach might be considered optimal for translation to a larger animal model or a potential clinical scenario. Alternatively, an adaptation of the transpedicular approach, as presented by Vadalà et al,[29] could offer a potential surgical path into the vertebra interior. The bone tissue comprising the vertebrae has a much higher intrinsic regenerative capacity, and as such, will likely be less affected by drill-hole or needle puncture defects than the IVD. Moreover, the bone marrow of the vertebrae is the natural environment of the MSC increasing the likelihood of their survival and integration, compared to the chemically- and mechanically harsh IVD-environment.

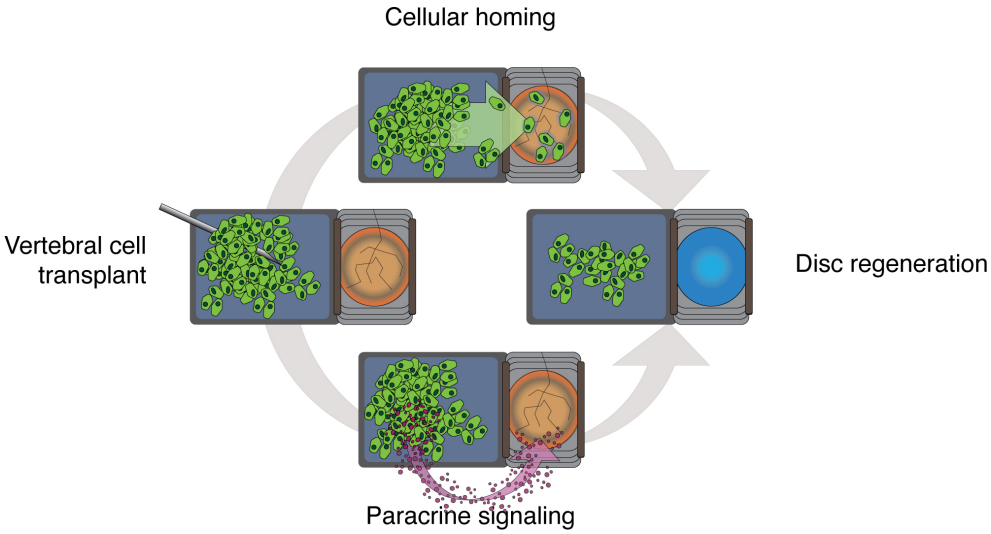

FIGURE 6 Hypothesized mechanisms. A schematic illustration on the potential regenerative mechanisms speculated to be involved in the observed regenerative outcomes of the vertebrally transplanted MSCs.

Altogether, our study emphasizes the potential of vertebral MSC transplantation, as a method to overcome concerns related with intradiscal cellular transplantation. Nevertheless, our study observed its beneficial effects in a relatively short time window. Further work is needed to confirm its long-term potential. Moreover, the translatability of the results in our rat model to a human scenario remains to be confirmed. Specifically, the rat IVD is hallmarked by differences in its dimensions, cell populations (predominantly notochordal cells instead of chondrogenic NP cells), endplate organization, and so forth.[25,27,57–61] Moreover, the model employed involves a more acute disc degeneration model rather than the commonly chronic degenerative processes involved in human discogenic pain.[58,62] How these differences might negatively or positively impact the therapeutic potential of a vertebral MSC transplantation strategy remains to be determined. Finally, our cells showed the capability of mitigating the induced IVD damage and migrating into the IVD, although the number of detected cells remained small. Whether these low numbers are sufficient for allowing direct support of disc maintenance remains unclear. Similarly, for intradiscal cell therapies, only a fraction of the transplanted cells can be found present in the disc upon transplantation,[13,40] but have been shown able to contribute to IVD matrix production.[63] However, questions remain whether the primary therapeutic effects of the de novo cells are derived from direct ECM product, paracrine signaling, or chemoattraction.[15] Similarly, for our vertebral MSC transplantation, whether cellular migration, paracrine signaling, or the combinations of both are the predominant beneficial factors remains to be determined and is a topic of future study. (Figure 6).

5 | CONCLUSIONS

Our study exhibits the potential of vertebral transplantation for the introduction of cellular therapeutics to limit the IVD degeneration cascade. This offers an alternative approach to deliver regenerative cell populations to potentially treat IVD diseases. Further investigation is needed to define the full potential and mechanism of vertebral cell transplantation as a treatment strategy for IVD repair.

AUTHOR CONTRIBUTIONS

Conception and design of the study; Jordy Schol, Daisuke Sakai, Takayuki Warita, Tadashi Nukaga, Kosuke Sako, Stephan Zeiter, Mauro Alini, and Sibylle Grad. Data acquisition and surgical performance; Jordy Schol, Takayuki Warita, Tadashi Nukaga, Kosuke Sako, Sebastian Wangler, and Shota Tamagawa. Data analysis: Jordy Schol Interpretation of the data; Jordy Schol, Daisuke Sakai, Stephan Zeiter, Mauro Alini, Sibylle Grad. Drafted initial version manuscript; Jordy Schol Critically revised the manuscript for intellectual content; Jordy Schol, Daisuke Sakai, Takayuki Warita, Tadashi Nukaga, Kosuke Sako, Sebastian Wangler, Stephan Zeiter, Stephan Zeiter, Mauro Alini, and Sibylle Grad. Study supervision: Jordy Schol, Daisuke Sakai, Mauro Alini, and Sibylle Grad. All authors approve the final version and agree to be accountable for all aspects of the work.

ACKNOWLEDGMENTS

We would like to acknowledge the support of the Support Center for Medical Research and Education at Tokai University with tissue processing and histological specimen preparation. Also, for the center's support in animal care and surgical assistance. We would also like to thank Professor Yutaka Inagaki (Dep. Innovative Medical Sciences, Tokai University School of Medicine, Japan) for kindly providing the transgenic mice.

FUNDING INFORMATION

This study was partially funded by a Bridging Grant from the Swiss State Secretariat for Education, Research, and Innovation (nr. BG03-092019) and by the AO Foundation and AO Spine.

CONFLICT OF INTEREST

TW is a paid employee of TUNZ Pharma Co. Ltd. (Osaka, Japan). DS is a scientific advisor of TUNZ Pharma Co. Ltd.

ORCID

Jordy Schol https://orcid.org/0000-0001-5489-2591
Daisuke Sakai https://orcid.org/0000-0003-4189-9270
Kosuke Sako https://orcid.org/0000-0002-4305-7774
Sebastian Wangler https://orcid.org/0000-0003-0166-5525
Shota Tamagawa https://orcid.org/0000-0002-5384-8158
Stephan Zeiter https://orcid.org/0000-0002-8155-4202
Mauro Alini https://orcid.org/0000-0002-0262-1412
Sibylle Grad https://orcid.org/0000-0001-9552-3653

REFERENCES

1. Vos T, Allen C, Arora M, et al. Global, regional, and national incidence, prevalence, and years lived with disability for 310 diseases and injuries, 1990–2015: a systematic analysis for the global burden of disease study 2015. *The Lancet*. 2016;*388*:1545-1602.
2. Stevans JM, Delitto A, Khoja SS, et al. Risk factors associated with transition from acute to chronic low Back pain in US patients seeking primary care. *JAMA Netw Open*. 2021;*4*:e2037371.
3. Takeoka Y, Yurube T, Nishida K. Gene therapy approach for intervertebral disc degeneration: an update. *Neurospine*. 2020;*17*:3-14.
4. Krupkova O, Cambria E, Besse L, et al. The potential of CRISPR/Cas9 genome editing for the study and treatment of intervertebral disc pathologies. *JOR Spine*. 2018;*1*:e1003.
5. Buckley CT, Hoyland JA, Fujii K, Pandit A, Iatridis JC, Grad S. Critical aspects and challenges for intervertebral disc repair and regeneration-harnessing advances in tissue engineering. *JOR Spine*. 2018;*1*:e1029.
6. De Pieri A, Byerley AM, Musumeci CR, Salemizadehparizi F, Vanderhorst MA, Wuertz-Kozak K. Electrospinning and 3D bioprinting for intervertebral disc tissue engineering. *JOR Spine*. 2020;*3*:e1117.
7. Clouet J, Vinatier C, Merceron C, et al. The intervertebral disc: from pathophysiology to tissue engineering. *Joint Bone Spine*. 2009;*76*:614-618.
8. Bowles RD, Setton LA. Biomaterials for intervertebral disc regeneration and repair. *Biomaterials*. 2017;*129*:54-67.
9. Hodgkinson T, Shen B, Diwan A, Hoyland JA, Richardson SM. Therapeutic potential of growth differentiation factors in the treatment of degenerative disc diseases. *JOR Spine*. 2019;*2*:e1045.
10. Zhang F, Wang S, Li B, Tian W, Zhou Z, Liu S. Intradiscal injection for the management of low back pain. *JOR Spine*. 2022;*5*:e1186.
11. Sakai D. Future perspectives of cell-based therapy for intervertebral disc disease. *Eur Spine J*. 2008;*17*(Suppl 4):452-458.
12. Schol J, Sakai D. Cell therapy for intervertebral disc herniation and degenerative disc disease: clinical trials. *Int Orthop*. 2019;*43*:1011-1025.
13. Williams RJ, Tryfonidou MA, Snuggs JW, Le Maitre CL. Cell sources proposed for nucleus pulposus regeneration. *JOR Spine*. 2021;*4*:e1175.
14. Vedicherla S, Buckley CT. Cell-based therapies for intervertebral disc and cartilage regeneration- current concepts, parallels, and perspectives. *J Orthop Res*. 2017;*35*:8-22.
15. Sakai D, Schol J, Watanabe M. Clinical development of regenerative medicine targeted for intervertebral disc disease. *Medicina (Kaunas)*. 2022;*58*:267.
16. Smith LJ, Silverman L, Sakai D, et al. Advancing cell therapies for intervertebral disc regeneration from the lab to the clinic: recommendations of the ORS spine section. *JOR Spine*. 2018;*1*:e1036.
17. Benneker LM, Andersson G, Iatridis JC, et al. Cell therapy for intervertebral disc repair: advancing cell therapy from bench to clinics. *Eur Cell Mater*. 2014;*27*:5-11.
18. Chan SC, Gantenbein-Ritter B. Intervertebral disc regeneration or repair with biomaterials and stem cell therapy--feasible or fiction? *Swiss Med Wkly*. 2012;*142*:w13598.
19. Fournier DE, Kiser PK, Shoemaker JK, Battie MC, Seguin CA. Vascularization of the human intervertebral disc: a scoping review. *JOR Spine*. 2020;*3*:e1123.
20. Loibl M, Wuertz-Kozak K, Vadala G, Lang S, Fairbank J, Urban JP. Controversies in regenerative medicine: should intervertebral disc degeneration be treated with mesenchymal stem cells? *JOR Spine*. 2019;*2*:e1043.
21. McDonnell EE, Buckley CT. Consolidating and re-evaluating the human disc nutrient microenvironment. *JOR Spine*. 2022;*5*:e1192.
22. Shalash W, Ahrens SR, Bardonova LA, Byvaltsev VA, Giers MB. Patient-specific apparent diffusion maps used to model nutrient availability in degenerated intervertebral discs. *JOR Spine*. 2021;*4*:e1179.
23. Carragee EJ, Don AS, Hurwitz EL, Cuellar JM, Carrino JA, Herzog R. 2009 ISSLS prize winner: does discography cause accelerated progression of degeneration changes in the lumbar disc: a ten-year matched cohort study. *Spine (Phila Pa 1976)*. 2009;*34*:2338-2345.
24. Glaeser JD, Tawackoli W, Ju DG, et al. Optimization of a rat lumbar IVD degeneration model for low back pain. *JOR Spine*. 2020;*3*:e1092.
25. Lai A, Gansau J, Gullbrand SE, et al. Development of a standardized histopathology scoring system for intervertebral disc degeneration in rat models: an initiative of the ORS spine section. *JOR Spine*. 2021;*4*:e1150.
26. Constant C, Hom WW, Nehrbass D, et al. Comparison and optimization of sheep in vivo intervertebral disc injury model. *JOR Spine*. 2022;*5*:e1198.
27. Wawrose RA, Couch BK, Dombrowski M, et al. Percutaneous lumbar annular puncture: a rat model to study intervertebral disc degeneration and pain-related behavior. *JOR Spine*. 2022;*5*:e1202.
28. Vadala G, Sowa G, Hubert M, Gilbertson LG, Denaro V, Kang JD. Mesenchymal stem cells injection in degenerated intervertebral disc: cell leakage may induce osteophyte formation. *J Tissue Eng Regen Med*. 2012;*6*:348-355.
29. Vadala G, De Strobel F, Bernardini M, Denaro L, D'Avella D, Denaro V. The transpedicular approach for the study of intervertebral disc regeneration strategies: in vivo characterization. *Eur Spine J*. 2013;*22*-(Suppl 6):S972-S978.
30. Croft AS, Illien-Junger S, Grad S, Guerrero J, Wangler S, Gantenbein B. The application of mesenchymal stromal cells and their homing capabilities to regenerate the intervertebral disc. *Int J Mol Sci*. 2021;*22*(7):3519.
31. Ullah M, Liu DD, Thakor AS. Mesenchymal stromal cell homing: Mechanisms and strategies for improvement. *iScience*. 2019;*15*:421-438.
32. Pereira CL, Teixeira GQ, Ribeiro-Machado C, et al. Mesenchymal stem/stromal cells seeded on cartilaginous endplates promote intervertebral disc regeneration through extracellular matrix remodeling. *Sci Rep*. 2016;*6*:33836.
33. Illien-Junger S, Pattappa G, Peroglio M, et al. Homing of mesenchymal stem cells in induced degenerative intervertebral discs in a whole organ culture system. *Spine (Phila Pa 1976)*. 2012;*37*:1865-1873.
34. Wangler S, Peroglio M, Menzel U, et al. Mesenchymal stem cell homing into intervertebral discs enhances the Tie2-positive progenitor cell population, prevents cell death, and induces a proliferative response. *Spine (Phila Pa 1976)*. 2019;*44*:1613-1622.
35. Sakai D, Nakamura Y, Nakai T, et al. Exhaustion of nucleus pulposus progenitor cells with ageing and degeneration of the intervertebral disc. *Nat Commun*. 2012;*3*:1264.
36. Sakai D, Schol J, Bach FC, et al. Successful fishing for nucleus pulposus progenitor cells of the intervertebral disc across species. *JOR Spine*. 2018;*1*:e1018.
37. Sakai D, Nishimura K, Tanaka M, et al. Migration of bone marrow-derived cells for endogenous repair in a new tail-looping disc degeneration model in the mouse: a pilot study. *Spine J*. 2015;*15*:1356-1365.

38. Zhang L, Chan C. Isolation and enrichment of rat mesenchymal stem cells (MSCs) and separation of single-colony derived MSCs. *J Vis Exp*. 2010;(37):1852.
39. Zhu H, Guo ZK, Jiang XX, et al. A protocol for isolation and culture of mesenchymal stem cells from mouse compact bone. *Nat Protoc*. 2010;*5*:550-560.
40. Hiraishi S, Schol J, Sakai D, et al. Discogenic cell transplantation directly from a cryopreserved state in an induced intervertebral disc degeneration canine model. *JOR Spine*. 2018;*1*:e1013.
41. Sakai D, Andersson GB. Stem cell therapy for intervertebral disc regeneration: obstacles and solutions. *Nat Rev Rheumatol*. 2015;*11*:243-256.
42. Issy AC, Castania V, Silveira JW, et al. Does a small size needle puncture cause intervertebral disc changes? *Acta Cirurgica Brasileira*. 2015;*30*:574-579.
43. Thomson AW, Bonham CA, Zeevi A. Mode of action of tacrolimus (FK506): molecular and cellular mechanisms. *Ther Drug Monit*. 1995;*17*:584-591.
44. Nagano J, Iyonaga K, Kawamura K, et al. Use of tacrolimus, a potent antifibrotic agent, in bleomycin-induced lung fibrosis. *Eur Respir J*. 2006;*27*:460-469.
45. Lan CC, Fang AH, Wu PH, et al. Tacrolimus abrogates TGF-beta1-induced type I collagen production in normal human fibroblasts through suppressing p38MAPK signalling pathway: implications on treatment of chronic atopic dermatitis lesions. *J Eur Acad Dermatol Venereol*. 2014;*28*:204-215.
46. Kugimiya F, Yano F, Ohba S, et al. Mechanism of osteogenic induction by FK506 via BMP/Smad pathways. *Biochem Biophys Res Commun*. 2005;*338*:872-879.
47. Wangler S, Menzel U, Li Z, et al. CD146/MCAM distinguishes stem cell subpopulations with distinct migration and regenerative potential in degenerative intervertebral discs. *Osteoarthr Cartil*. 2019;*27*:1094-1105.
48. Ying J, Han Z, Pei S, Su L, Ruan D. Effects of stromal cell-derived factor-1alpha secreted in degenerative intervertebral disc on activation and recruitment of nucleus pulposus-derived stem cells. *Stem Cells Int*. 2019;*2019*:9147835.
49. Pattappa G, Peroglio M, Sakai D, et al. CCL5/RANTES is a key chemoattractant released by degenerative intervertebral discs in organ culture. *Eur Cell Mater*. 2014;*27*:124-136.
50. Lapidot T, Kollet O. The essential roles of the chemokine SDF-1 and its receptor CXCR4 in human stem cell homing and repopulation of transplanted immune-deficient NOD/SCID and NOD/SCID/B2m(null) mice. *Leukemia*. 2002;*16*:1992-2003.
51. Centola M, Tonnarelli B, Scharen S, Glaser N, Barbero A, Martin I. Priming 3D cultures of human mesenchymal stromal cells toward cartilage formation via developmental pathways. *Stem Cells Dev*. 2013;*22*:2849-2858.
52. Morita K, Schol J, Volleman TNE, Sakai D, Sato M, Watanabe M. Screening for growth-factor combinations enabling synergistic differentiation of human MSC to nucleus pulposus cell-like cells. *Appl Sci*. 2021;*11*:3673.
53. Liao Z, Luo R, Li G, et al. Exosomes from mesenchymal stem cells modulate endoplasmic reticulum stress to protect against nucleus pulposus cell death and ameliorate intervertebral disc degeneration in vivo. *Theranostics*. 2019;*9*:4084-4100.
54. Niu CC, Yuan LJ, Lin SS, et al. Mesenchymal stem cell and nucleus pulposus cell coculture modulates cell profile. *Clin Orthop Relat Res*. 2009;*467*:3263-3272.
55. Strassburg S, Hodson NW, Hill PI, Chen LH, Chen WJ. Bi-directional exchange of membrane components occurs during co-culture of mesenchymal stem cells and nucleus pulposus cells. *PLoS One*. 2012;*7*:e33739.
56. Strassburg S, Richardson SM, Freemont AJ, et al. Co-culture induces mesenchymal stem cell differentiation and modulation of the degenerate human nucleus pulposus cell phenotype. *Regen Med*. 2010;*5*:701-711.
57. Lillyman DJ, Lee FS, Barnett EC, et al. Axial hypersensitivity is associated with aberrant nerve sprouting in a novel model of disc degeneration in female Sprague Dawley rats. *JOR Spine*. 2022;*5*(3):e1212.
58. Barcellona MN, McDonnell EE, Samuel S, et al. Rat tail models for the assessment of injectable nucleus pulposus regeneration strategies. *JOR Spine*. 2022;*5*(3):e1216.
59. Lakstins K, Arnold L, Gunsch G, et al. Characterization of bovine and canine animal model cartilage endplates and comparison to human cartilage endplate structure, matrix composition, and cell phenotype. *JOR Spine*. 2020;*3*:e1116.
60. Alini M, Eisenstein SM, Ito K, et al. Are animal models useful for studying human disc disorders/degeneration? *Eur Spine J*. 2008;*17*:2-19.
61. Li YH, Wu HL, Li Z, et al. Species variation in the cartilaginous endplate of the lumbar intervertebral disc. *JOR Spine*. 2022;*5*(3):e1218.
62. He S, Zhang Y, Zhou Z, et al. Similarity and difference between aging and puncture-induced intervertebral disc degeneration. *J Orthop Res*. 2022;*40*(11):2565-2575.
63. Henriksson HB, Papadimitriou N, Hingert D, et al. The traceability of mesenchymal stromal cells after injection into degenerated discs in patients with low Back pain. *Stem Cells Dev*. 2019;*28*:1203-1211.

SUPPORTING INFORMATION

Additional supporting information can be found online in the Supporting Information section at the end of this article.

How to cite this article: Schol, J., Sakai, D., Warita, T., Nukaga, T., Sako, K., Wangler, S., Tamagawa, S., Zeiter, S., Alini, M., & Grad, S. (2023). Homing of vertebral-delivered mesenchymal stromal cells for degenerative intervertebral discs repair – an in vivo proof-of-concept study. *JOR Spine*, *6*(1), e1228. https://doi.org/10.1002/jsp2.1228